ENVIRONMENTAL RESEARCH
COMMUNICATIONS

LETTER • OPEN ACCESS

Attribution of air temperature and precipitation to the future global drought events

To cite this article: Rui Fu *et al* 2023 *Environ. Res. Commun.* **5** 061005

Environmental Research Communications

OPEN ACCESS

RECEIVED
29 January 2023

REVISED
3 June 2023

ACCEPTED FOR PUBLICATION
13 June 2023

PUBLISHED
26 June 2023

LETTER

Attribution of air temperature and precipitation to the future global drought events

Rui Fu[1], **Changjing Wang**[1], **Dujuan Ma**[1], **Hongfan Gu**[1], **Qiaoyun Xie**[2], **Guoxiang Liu**[1] and **Gaofei Yin**[1]

[1] Faculty of Geosciences and Environmental Engineering, Southwest Jiaotong University, Chengdu 610031, People's Republic of China
[2] School of Engineering, the University of Western Australia, Perth, WA 6009, Australia

E-mail: yingf@swjtu.edu.cn

Keywords: drought event, precipitation, air temperature, CMIP6, contribution, climate change

Abstract

Quantifying the contributions of air temperature and precipitation changes to drought events can inform decision-makers to mitigate the impact of droughts while existing studies focused mainly on long-term dryness trends. Based on the latest Coupled Model Intercomparison Project (CMIP6), we analyzed the changes in drought events and separated the contributions of air temperature and precipitation to the risk of future drought events. We found that drought frequency, duration, severity, and month will increase in the future (56.4%, 63.5%, 82.9%, and 58.2% of the global land area in SSP245, and 58.1%, 67.7%, 85.8%, and 60.5% of the global land area in SSP585, respectively). The intermediate scenario has a similar pattern to the most extreme scenario, but low emission was found to mitigate drought risk. Globally, we found that air temperature will have a greater impact than precipitation on intensifying drought. Increasing precipitation will mitigate drought risks in some middle and high northern latitudes, whilst the trend in increasing air temperature will counter the effects of precipitation and increase the impact of droughts. Our study improves the understanding of the dynamics of future devastating drought events and informs the decision-making of stakeholders.

1. Introduction

Drought reduces gross primary production, incurs vegetation mortality, and therefore affects the terrestrial carbon cycle Green *et al* 2019, Van der Molen *et al* (2011), resulting in multifaceted challenges in drinking water security, agriculture, and the economy (Park *et al* 2016). Devastating drought events, therefore, have attracted widespread attention and discussion across Australia (Araujo *et al* 2022), the Horn of Africa (Funk *et al* 2019), and southwest China (Song *et al* 2019, Wang *et al* 2021) amongst others. A critical goal within the scientific community is to advance knowledge of drought events to inform decision-making regarding drought events. Unravelling the drivers of drought events and how these drivers affect droughts under ongoing climate warming is therefore a compelling scientific question of widespread importance.

The frequency, duration, and intensity of global drought events are expected to increase under future predicted warming (Dai *et al* 2018, Zhang *et al* 2019, Christian *et al* 2021). The main cause of the drought was often assumed to be the lack of precipitation (Ukkola *et al* 2020, Mckee *et al* (1993)). It is widely reported that precipitation will increase in the central Sahel, eastern Russia, northern China, and northern high latitudes (Ukkola *et al* 2020, Zhao and Dai 2021). In theory, the increasing precipitation should ease the droughts in these regions. Precipitation, however, does not represent the only climatic factor controlling drought. Temperature is also a key determinant, given that climate warming exponentially stimulates potential evapotranspiration (PET) (Mcvicar *et al* (2012), Beguería et al 2014, Vicente-Serrano *et al* 2010, Vicente-Serrano *et al* 2015, Zeng *et al* 2020, Xu *et al* 2021a, Thornthwaite 1948, Allen *et al* 1998). It, therefore, seems to be necessary to consider the effect of climatic warming on drought events (Vicente-Serrano *et al* 2010, Frierson and Scheff 2014, Zhao and Dai 2015, Zhao and Dai 2021).

Table 1. CMIP6 models used in this study.

Model	Resolution (longitude × latitude)	References
ACCESS-CM2	2.5° × 2.5°	(Dix *et al* 2019a, 2019b)
ACCESS-ESM1-5	2.5° × 2.5°	(Ziehn *et al* 2019a, 2019b)
BCC-CSM2-MR	1° × 1.125°	(Xin *et al* 2019a, 2019b)
CanESM5	2.8125° × 2.8125°	(Swart *et al* 2019a, 2019b)
EC-Earth3	1.40625° × 1.40625°	(Consortium 2019c, 2019d)
EC-Earth3-Veg	1.875° × 1.875°	(Consortium 2019a, 2019b)
FGOALS-f3-L	2.8125° × 3°	(Yu 2019a, 2019b)
GFDL-ESM4	1.25° × 1°	(John *et al* 2018a, 2018b)
INM-CM4-8	1.875° × 1.241°	(Volodin *et al* 2019a, 2019b)
INM-CM5-0	1.875° × 1.241°	(Volodin *et al* 2019c, 2019d)
IPSL-CM6A-LR	3.75° × 1.8945°	(Boucher *et al* 2019a, 2019b)
MIROC6	1.25° × 1.25°	(Shiogama *et al* 2019a, 2019b)
MPI-ESM1-2-HR	1.25° × 1.25°	(Schupfner *et al* 2019a, 2019b)
MPI-ESM1-2-LR	1.25° × 1.25°	(Wieners *et al* 2019a, 2019b)
MRI-ESM2-0	1° × 1.125°	(Yukimoto *et al* 2019a, 2019b)

The precipitation and temperature variability are the main factors that directly affect the change trends of dryness/wetness (Alexander *et al* 2006, Hance *et al* 2007, Liu *et al* 2009, Wang *et al* 2016, Wu and Chen 2019). The idea of evaluating the relative contributions from changes in moisture supply (precipitation) versus evaporative demand (PET), mainly depending on temperature (Arora and Boer 2001, Sun *et al* 2016, Hui-Mean *et al* 2018), to drought index is not new. For instance, Feng and Fu (2013) examined the contributions of precipitation and PET to projected changes in the P/PET ratio. By using different drought indexes, they found a widespread dryness trend in the twenty-first century because of increased PET and reduced precipitation over subtropical areas (Cook *et al* 2014, Zhao and Dai 2015, Cook *et al* 2020, Zhao and Dai 2021). A key conceptual issue is to distinguish drought events and long-term aridity trends (Sherwood and Fu 2014). Existing studies focused mainly on long-term aridity trends, rather than drought events.

In this study, we focus on agricultural drought events, which often defined as soil water deficiency caused by long-term meteorological drought (Vicente-Serrano *et al* 2010, Beguería *et al* 2014, Sherwood and Fu 2014). Unravelling the drivers of drought development not only improves our understanding about future drought dynamics but also informs the decision-making of stakeholders to reduce the losses caused by droughts. To date, few works have quantitatively separated the contributions of precipitation and PET to future drought event changes (Zhang *et al* 2019, Wang *et al* 2022). These progress in drought events attribution researches are via past and regional analyses, a key scientific question remains: To what extent will climate change affect global drought events in the future? To address this question, we characterize the spatiotemporal dynamics of future agricultural drought events and separate the contributions of air temperature and precipitation on these dynamics.

2. Materials and methods

2.1. Data

We obtained monthly simulations of total precipitation, surface air minimum temperature (T_{min}) and maximum temperature (T_{max}) from the Coupled Model Intercomparison Project phases 6 (CMIP6). Fifteen climate models were used and averaged to eliminate the uncertainty of artificial factors and model selection (table 1). To compare the difference between historical and future global drought events, we used the historical experiment (1850–2014) and two future scenarios (2015–2100) including Shared Socioeconomic Pathways (SSP) 2-4.5 and 5-8.5. SSP 245 represents an intermediate 'middle of the road' future climate scenario and SSP 585 is a high emissions 'fossil-fueled development' future scenario O'neill *et al* (2016). We re-gridded all data into 2 × 2° through the bilinear interpolation.

We utilized the 2020 MODIS Land Cover Type Yearly Climate Modeling Grid (MCD12C1.006 product) to mask the desert areas, since it is difficult to assess droughts in places where zero-precipitation amounts are the norm. MCD12C1 dataset was acquired from https://lpdaac.usgs.gov/products, which offers aggregated land cover data at a resolution of 0.05°.

Table 2. Information about the simulated experiments in this study.

Experiment	Abbreviation	Data period	
		Precipitation	Air temperature
$P_{2031–2060} - PET_{2031–2060}$	S1	2031–2060	2031–2060
$P_{2031–2060} - PET_{1981–2010}$	S2	2031–2060	1981–2010
$P_{1981–2010} - PET_{2031–2060}$	S3	1981–2010	2031–2060

2.2. Drought definition

Many definitions of drought exist. Here we consider agricultural droughts. as the 3-month scale SPEI can satisfactorily capture the vegetation response to drought (Lloyd-Hughes 2012, Xu *et al* 2015), it has been widely used in monitoring and assessing agriculture drought (Li *et al* 2019, Wang *et al* 2021, Zeng *et al* 2021).

Using percentile thresholds to determine drought periods is a common approach in hydrology and climatology (Trenberth *et al* 2014, Ukkola *et al* 2020). One advantage of this method is that it does not rely on any assumptions about the data distribution. This makes it more robust to outliers or non-normal data distributions. To better compare with Ukkola's work, precipitation minus potential evapotranspiration (P − PET) was used in our study to quantify the characteristics of drought.

PET was calculated by precipitation, extraterrestrial radiation, $T_{min,}$ and T_{max} based on the modified Hargreaves equation. The modified Hargreaves equation considers multiple relevant variables affecting PET, which is more reliable than the single variable method (Xu *et al* 2021a). The modified Hargreaves equation has shown similar results to the Penman-Monteith method (Droogers and Allen 2002, Beguería *et al* 2014, de Streel *et al* 2022). According to Droogers and Allen (2002), PET is calculated as:

$$PET = 0.0013 \times 0.408R_a \times (T_{avg} + 17.0) \times (TD - 0.0123P)^{0.76} \quad (1)$$

where R_a is the extraterrestrial radiation (can be estimated from the latitude and the month of the year); T_{avg} is the monthly average temperature; TD is the temperature range, calculated as the difference between daily maximum temperature and minimum temperature; P is precipitation in mm per month. To consider the effects of temperature changes individually, we fixed the change in precipitation at 0 and calculated R_a using the latitude and the month of the year in this study.

We converted the monthly P − PET time series into 3-month accumulations to smooth out short-term variations. This is analogous to calculating the Standardized Precipitation Evapotranspiration Index (SPEI) at the time-scale of 3 months and reflects changes in seasonal droughts, which can satisfactorily capture the vegetation response to drought and the characteristics of short-term variations in soil moisture (Lloyd-Hughes 2012, Xu *et al* 2015).

Quantifying drought in percentiles, rather than mean values, provides a better description of drought characterization. Percentile thresholds involve no assumptions about the data distribution. In this study, the 10th percentile thresholds (x_{10m}; mm) were defined separately for each month from the 3-month accumulated P − PET to account for seasonality, then any month below these thresholds is classified as drought. The 10th percentile corresponds approximately to severe drought. The monthly 10th percentile thresholds were derived from the period 1980−2014. Subsequently, we calculated three common drought characteristics (duration, frequency and severity), and drought month. Drought month would provide a more realistic and comprehensive estimate of the temporal exposure to drought in different regions than frequency or duration alone. Drought frequency, duration and severity is focus more on characteristics of drought events. Drought events were first identified by the start and end months of the drought, and then their duration and severity were then determined. The number of continuous drought months is defined as the duration of a drought event. Severity (mm $month^{-1}$) was calculated by averaging the difference between the drought threshold and the monthly 3-month accumulation P − PET value (x_m; mm) over all months during the drought event. Frequency refers to the number of drought events over a period. Drought months is the product of duration and frequency.

2.3. Attribution of the drought event

We designed some simulated experiments to separate the respective contributions of the air temperature and precipitation for future P—PET (table 2). We first calculated the $P_{2031–2060} - PET_{2031–2060}$ (S1) during 2031 and 2060 in the two future scenarios (SSP 245 and SSP 585), and defined the S1 as the baseline case. Secondly, the $P_{2031–2060} - PET_{1981–2010}$ (S2) and $P_{1981–2010} - PET_{2031–2060}$ (S3) were obtained by replacing with past (1981–2010) temperature and precipitation, respectively. Compared with S1, S2 represents the P − PET with past temperature but with future precipitation, while S3 represents P − PET with past precipitation and future air temperature. Thirdly, we calculated drought characteristics in S1, S2, and S3. Finally, the contribution of the air temperature to the future drought was the difference in drought characteristics between S1 and S2 (S1–S2),

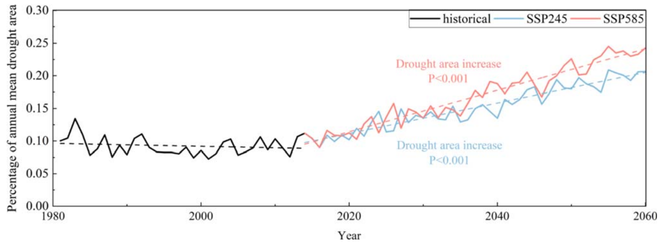

Figure 1. The temporal curves of percentage of annual average drought area (drought cells divide total cells) in different scenarios. Black color stands for the historical annual average drought area, blue color for the SSP 245 and red color for SSP 585.

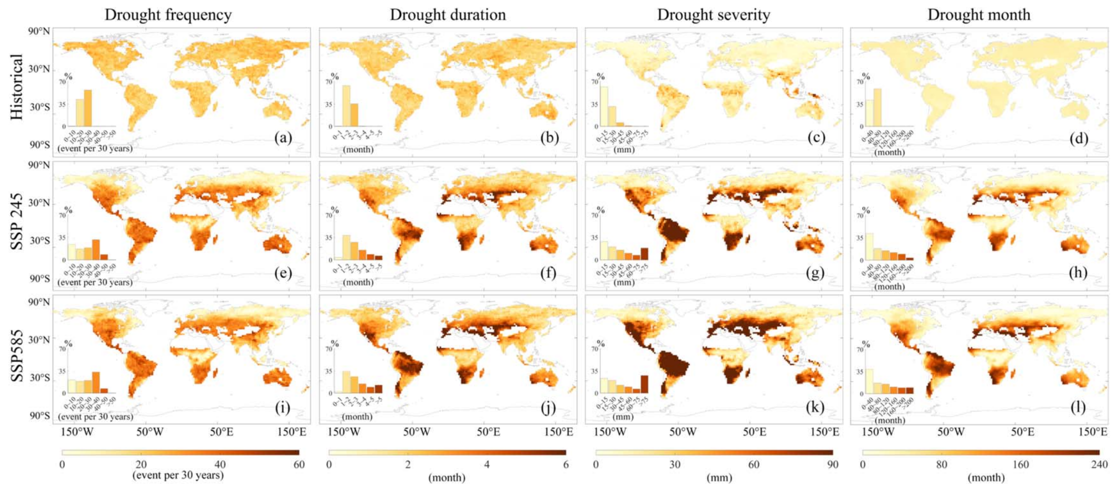

Figure 2. Spatial distributions in historical (1981–2010) and future (2031–2060) drought characteristics. Drought frequency (the first column), duration (the second column), severity (the third column), and month (the fourth column) were employed to quantify the drought event. The historical (the first row) and future cases (the second and third rows for the SSP245 and 585 scenarios, respectively) were calculated with the multi-model averaged precipitation and potential evapotranspiration in CMIP6 simulations. The inset in each subplot represents the corresponding probability distribution.

and the contribution of precipitation to the future drought was defined as the difference in drought characteristics between S1 and S3 (S1—S3). In addition, we defined a positive contribution as increasing drought event characteristics and a negative contribution as decreasing drought event characteristics.

3. Results

3.1. Projected changes in drought characteristics

The long-term series of percentage of annual average drought area (PAADA) (drought cells divide total cells) from 1981 to 2060 is presented in figure 1. The annual average drought area in the SSP 585 scenario was temporally consistent with the SSP 245 scenario before 2030, whereas significantly higher than the SSP 245 scenario after 2030. In addition, the PAADA showed significant increase trends (0.024 decade^{-1} and 0.032 decade^{-1} for SSP 245 and SSP 585, respectively) in the future while the historic trend showed no significant trend. These indicate that the global drought is increasing and will intensify in the future.

Figure 2 shows the drought distribution in the past and two future scenarios. As for the historical period (figures 2(a)–(d)), the global drought frequency, duration and month were spatially homogeneous (figures 2(a) (b), and (d)). But the tropical and subtropical regions experienced more severe droughts (figure 2(c)). In 2031–2060, most tropical and subtropical regions, including Amazon, Australia, Central America, Central Asia, Chile, the Mediterranean, and southern Africa, are projected to experience longer, more frequent, and stronger droughts, especially in the SSP 585 scenario (figures 2(i)–(l)). Although drought frequency has only increased by less than one time, it is noteworthy that the drought months have generally increased by more than two times, and even increased by more than fivefold in the most severe regions.

To directly compare the difference between the past and future cases, we subtracted historical drought features from future ones (figure 3). Firstly, the strongest frequency increases are expected to occur in most

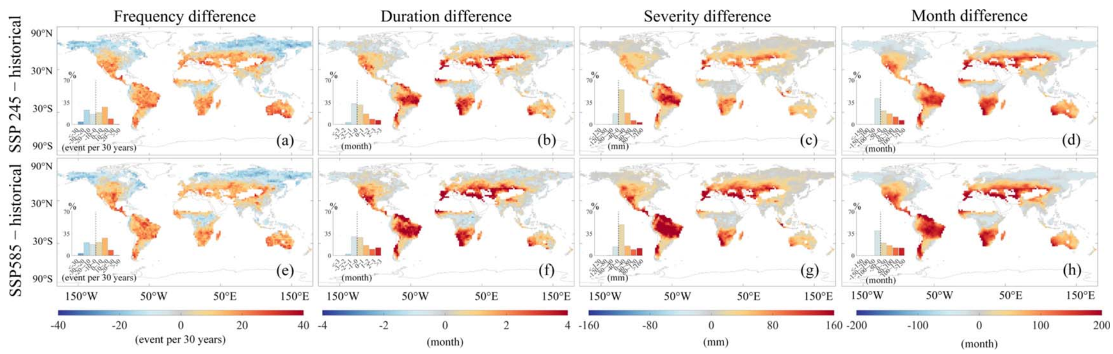

Figure 3. The difference in drought frequency (the first column), duration (the second column), severity (the third column), and month (the fourth column) between future (2031–2060) and historical (1981–2010) cases. SSP 245 and 585 were respectively used for the first and second rows. The inset in each subplot represents the corresponding probability distribution.

tropical and subtropical regions, with increases in drought frequency from ~20 during the historical period to ~40 in the future (figures 3(a) and (e)). By contrast, the drought frequency is projected to decrease by up to 20 in northern high latitudes. As for duration and severity, Amazon, Central Asia, Chile, the Mediterranean, southern Africa, and western Australia showed larger changes than other places (figures 3(b), (c), (f), and (g)). Their duration extended from ~2 months during the historical period to ~6 months in the SSP 245 and over 6 months in the SSP 585. Drought month, represents total number of drought months over 30 years, showed similar and more continuous pattern with drought frequency and duration. Although the frequency of droughts has increased by less than 100%, it is noteworthy that the number of drought months has generally increased by more than two times, and in the most severely affected areas, it has even increased by more than five times. This means that the risk of prolonged drought events in hotspots is greatly increased.

There are large global land areas of increased drought frequency (SSP 245 = 56.4%, SSP 585 = 58.1%), duration (SSP 245 = 63.5%, SSP 585 = 67.7%), severity (SSP 245 = 82.9%, SSP 585 = 85.8%), and month (SSP 245 = 58.2%, SSP 585 = 60.5%). This indicates that many regions, including almost all low and middle latitudes, will experience longer and more serious drought events, while droughts in the northern high latitudes will be eased. The overall pattern of drought frequency difference was similar between SSP 245 and SSP 585, but drought duration and severity in SSP 585 showed a larger difference than those in SSP 245.

3.2. Contributions of air temperature and precipitation

The temporal curves of PAADA, in different simulations, from 2031 to 2060 are presented in figure 4. The PAADA in $P_{1981–2010} - PET_{2031–2060}$ (S3) is closer to the PAADA in $P_{2031–2060} - PET_{2031–2060}$ (S1) than PAADA in $P_{2031–2060} - PET_{1981–2010}$ (S2) (figures 4(a) and (b)), implying changes in air temperature will have a greater impact on future drought events than precipitation. Close inspection revealed air temperature and precipitation would exert contrasting influences on future drought (negative and positive, respectively), and precipitation and air temperature in SSP 585 contributed more than those in SSP 245 (figure 4(c)).

In SSP 245 and SSP 585, the PAADA in S1 (SSP 245: 0.026 decade^{-1}, SSP 585: 0.035 decade^{-1}) and PAADA in S2 (SSP 245: 0.018 decade^{-1}, SSP 585: 0.023 decade^{-1}) showed significant increase trends. This indicates that the contribution of air temperature for PAADA increases in the future. Specifically, contribution of air temperature for PAADA will increase 0.009 per decade in SSP 245 and 0.012 per decade in SSP 585. While the mitigation effect of precipitation for PAADA will be decreased in the future (0.023 decade^{-1} in SSP 245 and 0.014 decade^{-1} in SSP 585).

We also analyzed the distribution of the contributions of air temperature and precipitation for drought frequency, duration, severity, and month. In terms of the drought frequency (figures 5(a)–(d)), air temperature strongly increases the future drought frequency (96.4% and 92.2% of the global land area in SSP 245 and SSP 585, respectively) (figures 5(a) and (b)). While the precipitation decreases drought frequency in Canada, northern China, Russia, and other high latitude regions (in total, 75.1% and 75.9% of the global land area in SSP 245 and 585, respectively) (figures 5(b) and (f)), and increases drought events in Amazon, Australia, Central America, Central Asia, Chile, northwest China, and southern Africa, in line with previous studies (figures 5(c) and (d)).

Air temperature increases generally extend the future drought duration (91.4% and 92.4% of the global land area in SSP 245 and SSP 585, respectively). Precipitation will extend the future drought duration in northern high latitudes while shortening the future drought duration in most low and middle latitudes (62.7% and 64.8% of the global land area in SSP 245 and SSP 585, respectively). In addition, air temperature increases strongly

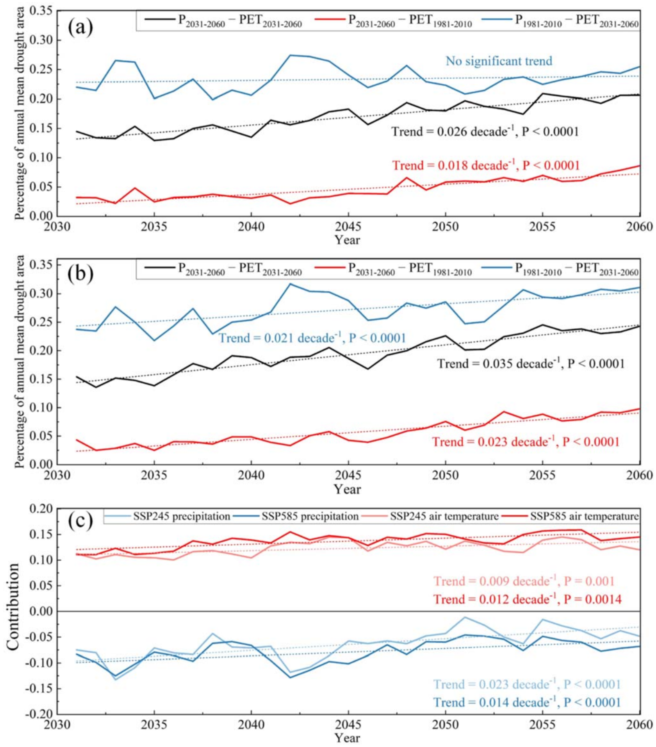

Figure 4. The temporal curves of future (2031–2060) percentage of annual average drought area (PAADA) in different simulations from 2031 to 2060, in (a) SSP 245 and (b) 585 scenarios, and (c) the temporal curves of the contribution of air temperature and precipitation for PAADA in SSP 245 and 585. The CMIP6 simulated future and historical (1981–2010) P ($P_{2031–2060}$ and $P_{1981–2010}$, respectively) and PET ($PET_{2031–2060}$ and $PET_{1981–2010}$, respectively) were all used to calculate P − PET. The contribution of precipitation to the future drought can be represented by the difference between $P_{2031–2060} - PET_{2031–2060}$ and $P_{1981–2010} - PET_{2031–2060}$. The contribution of air temperature was calculated similarly but with $PET_{1981–2010}$, which was calculated with historical air temperature.

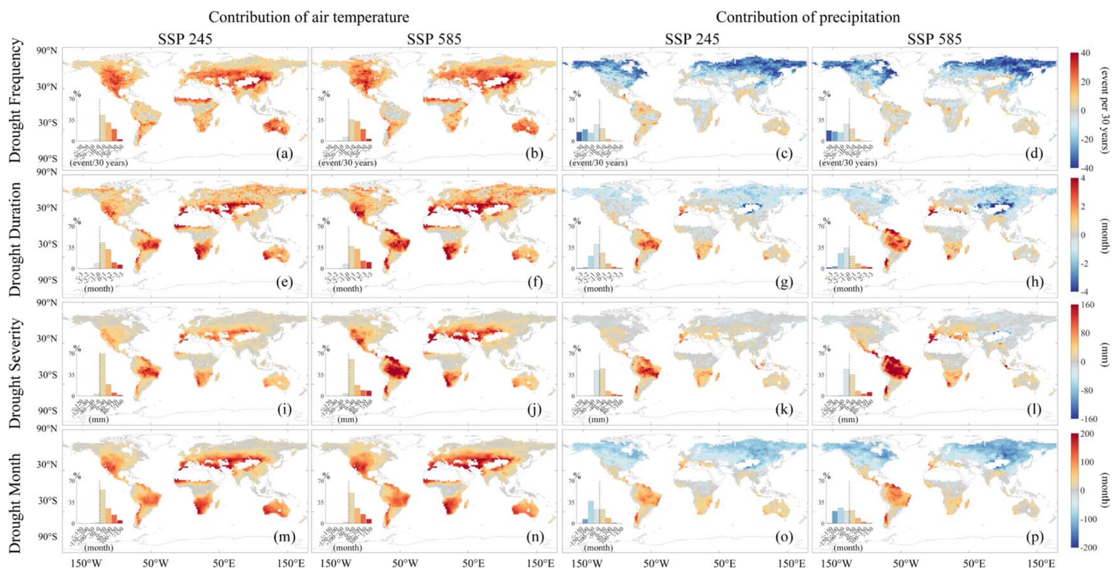

Figure 5. Contributions of air temperature (the first and second columns) and precipitation (the third and fourth columns) to future drought frequency (the first row), duration (the second row), severity (the third row), and month (the fourth row). SSP 245 was used for the first and third columns, and SSP 585 was used for the second and fourth columns. The inset in each subplot represents the corresponding probability distribution.

extend drought duration over 2 months in 16.6% of the global land area (figures 5(e)) and 23.5% (figure 5(f)) in Central Asia, Chile, the Mediterranean, southern Africa, and western Australia. These results indicate that precipitation has less influence than the air temperature. The contributions of air temperature and precipitation to drought severity (figures 5(i)–(l)) follow a very similar pattern. (figures 5(e)–(h)).

Drought month provide a more realistic and comprehensive estimate of the temporal exposure to drought in different regions than frequency or duration alone. Although the direction of change is similar, drought month showed much more continuous pattern than drought frequency and duration. Changes in air temperature nearly leads to increase in global drought month (98.5% and 97.4% of the global land area in SSP 245 and SSP 585, respectively), which is more than that in drought frequency and duration. Overall, drought frequency, duration, and severity were increasing globally by air temperature and decreasing by precipitation except in Australia, Chile, the Mediterranean, southern Africa, and the western United States.

4. Discussion

Long-term dryness trend and its attribution are an active research area (Cook *et al* 2014, Frierson and Scheff 2014, Vicente-Serrano *et al* 2015, Zhao and Dai 2015, Wang *et al* 2022). The dryness trend, however, does not physically the same as drought events. A drought event is a transient regional phenomenon often defined as deviations from assumed known local climate norms (Sherwood and Fu 2014). Drought events were affected by both the change in mean-state (long-term dryness) and variability (Trenberth *et al* 2014, Zhang *et al* 2019, Ukkola *et al* 2020). Drought events and long-term dryness trends have different impacts on ecosystems. For instance, since decreased available water limits plant photosynthesis and transpiration, and increased radiation could promote photosynthesis (Jeong *et al* 2017, Zhang *et al* 2020, Yang *et al* 2022), dryness may cause complex impacts on vegetation (Jiao *et al* 2021). While devastating drought events could incur vegetation mortality, and therefore affects the terrestrial carbon cycle (Green *et al* 2019, Van der Molen *et al* (2011)), resulting in multifaceted challenges in drinking water security, agriculture, and the economy (Park *et al* 2016). Therefore, Ukkola *et al.* (2020) based on precipitation investigated changes of drought events globally. However, evaporative demand affected by ongoing air temperature can also play a critical role (Beguería *et al* 2014, Cook *et al* 2014, Zhao and Dai 2021). To date, few works have quantitatively separated the contributions of precipitation and PET to future drought event changes (Zhang *et al* 2019).

This study evaluated the future PAADA and drought event changes including drought frequency, duration, severity and month, and the respective contributions of air temperature and precipitation to drought event changes. If we only consider the contribution from precipitation, drought events would intensify in low and middle latitudes such as Amazon, Chile, the Mediterranean, and southern Africa, while easing in high latitudes (figures 5(c)–(d), (g)–(h), (k)–(l) and (o)–(p)), consistent with Ukkola *et al.* (2020). Generally, the increasing precipitation would ease the drought events on the global scale (Cook *et al* 2020, Wu *et al* 2022). However, the ongoing warming can cause higher PET, which would compensate or even reverse the mediation of drought by increasing precipitation, examples can be observed in central China and central and western United States. By separating the contributions of air temperature and precipitation to the risk of future drought events, our results advance the current understanding of future drought events and their drivers.

There is an unexpected but plausible phenomenon. The patterns of the contribution of air temperature to drought events are not identical to that of the overall air temperature trend. The air temperature will increase substantially at high latitudes, yet moderately at low latitudes under climate change (IPCC 2013). But changes in droughts contributed by air temperature in middle and low latitude regions are stronger than in high latitude regions (figures 5(a)–(b), (e), (f), (i)–(j) and (m)–(n)), which is similar to LIU et al (2020), Vicente-Serrano *et al* (2015), Cook *et al* (2014). This is because the relationship between PET and air temperature is non-linear, and the sensitivity of PET to air temperature is slight in cold conditions, e.g., in high latitude regions (Thornthwaite 1948, Hargreaves and engineering, 1994, Droogers and Allen 2002). This means that the droughts most affected by temperature were mainly distributed in the low and middle latitudes, instead of the high latitudes.

The CMIP6 model provides more reliable estimates compared with the CMIP5 model for future climate scenarios (O'neill *et al* (2016), Zelinka *et al* 2020) because the new general circulation models in CMIP6 capture the characteristics of large-scale patterns of precipitation well (Xin *et al* 2020, Xu *et al* 2021b). Besides, CMIP6 considered not only the carbon emission path but also social development factors such as population and Gross Domestic Product (Zelinka *et al* 2020, Xu *et al* 2021b). This will help to evaluate the drought characteristics affected by human activities and climate change. SSP 245 and SSP 585 represent intermediate and the most extreme scenarios with the driving force of about 4.5 W m^{-2} and 8.5 W m^{-2} (Canturk and Kulaç 2021), and results in this study showed that SSP 245 has a consistent pattern with SSP 585. However, drought events under the SSP 585 scenario showed longer durations with stronger severity than drought events under the SSP 245 scenario (figure 4), indicating that future changes in drought duration and severity will be affected by the intensity of greenhouse gas emissions. Therefore, lower greenhouse gas emissions would mitigate future drought events.

Given the critical role of diverse meteorological and climatological features in the drought development, it is imperative for future studies to employ multiple drought metrics, such as runoff and soil moisture, to comprehensively understand the drivers of drought intensification across the globe. Reasonable assumptions can improve the robustness of the method, making it more resistant to outliers (Guttman 1999, Pieper *et al* 2020). Additionally, using a distribution function other than the normal distribution expands the method's applicability to non-normal data distributions. In essence, fitting an appropriate distribution function to the time series of precipitation (and water balance) improves the characterization of extreme values in their respective distributions (Hayes *et al* 2011). Statistically improving the description of the tails of distributions is particularly important for the proper statistical treatment of extreme events. Besides, adhering to the drought index recommendation by the World Meteorological Organization can enhance comparability.

Moreover, there is a need for research that disentangles the complex interactions between drought and socioeconomic impacts. The results of this study can serve as a reference framework for quantifying the sensitivity of droughts. While the drivers of predicted drought are presented, further work is required to advance and validate the risk of drought development.

5. Conclusions

We compared drought events in the historical period (1981–2010) with two future (2031–2060) climate scenarios (SSP 245 and SSP 585) and attributed the contributions of future air temperature and precipitation to future drought events. Monthly climate data from fifteen CMIP 6 monthly models were applied to model the P − PET across the globe. The results can be summarized as follows:

(1) Drought frequency, duration, severity, and month will increase in most regions in the future (56.4%, 63.5%, 82.9%, and 58.2% of the global land area in SSP245, and 58.1%, 67.7%, 85.8%, and 60.5% of the global land area in SSP585, respectively). Importantly, drought events in the SSP 585 scenario showed longer durations and stronger severity than that in SSP 245, therefore, future changes in drought could be mitigated through lower greenhouse gas emissions.

(2) Future precipitation will ease the drought events in Canada, China, and northern high-latitude regions, while intensifying drought events in the Amazon, Australia, Central America, Chile, the Mediterranean, and southern Africa. Air temperature trends would exacerbate these drought events. Low and middle latitudes where precipitation is declining are more vulnerable to drought than areas with increased precipitation.

Overall, we provided a comprehensive and systematic way to quantify the risks and impacts of future drought events. As important drivers of drought, our results highlight how precipitation and air temperature will change drought characteristics. This offers a basis for strategies to cope with the risk of intensifying drought, and enhance water and food security in the future, despite uncertainty in precipitation and air temperature.

Acknowledgments

This research was funded by the Sichuan Science and Technology Program (2021JDJQ0007; 2020JDTD0003), and the National Natural Science Foundation of China (41971282). Qiaoyun Xie acknowledges support from University of Technology Sydney Chancellor's Postdoctoral Research Fellowship.

Data availability statement

The data that support the findings of this study are openly available at the following URL/DOI: https://doi.org/ https://esgf-node.llnl.gov/projects/cmip6/.

ORCID iDs

Rui Fu https://orcid.org/0000-0003-3298-8976
Hongfan Gu https://orcid.org/0000-0001-8612-7253
Qiaoyun Xie https://orcid.org/0000-0002-1576-6610

Gaofei Yin https://orcid.org/0000-0002-9828-7139

References

Alexander L V, Zhang X, Peterson T C, Caesar J, Gleason B, Klein Tank A, Haylock M, Collins D, Trewin B and Rahimzadeh F 2006 Global observed changes in daily climate extremes of temperature and precipitation *Journal of Geophysical Research: Atmospheres* **111** D5

Allen R G, Pereira L S, Raes D and Smith M J F 1998 Crop evapotranspiration-guidelines for computing crop water requirements-FAO irrigation and drainage paper 56. *Fao* **300** D05109

Araujo D S A, Marra F, Merow C and Nikolopoulos E I 2022 Today's 100 year droughts in Australia may become the norm by the end of the century *Environ. Res. Lett.* **17** 044034

Arora V K and Boer G J 2001 Effects of simulated climate change on the hydrology of major river basins *Journal of Geophysical Research: Atmospheres* **106** 3335–48

Beguería S, Vicente-Serrano S M, Reig F and Latorre B 2014 Standardized precipitation evapotranspiration index (SPEI) revisited: parameter fitting, evapotranspiration models, tools, datasets and drought monitoring *Int. J. Climatol.* **34** 3001–23

Boucher O *et al* 2019a IPSL IPSL-CM6A-LR model output prepared for CMIP6 ScenarioMIP ssp245 *Earth System Grid Federation* (https://doi.org/10.22033/ESGF/CMIP6.5264)

Boucher O *et al* 2019b IPSL IPSL-CM6A-LR model output prepared for CMIP6 ScenarioMIP ssp585 *Earth System Grid Federation* (https://doi.org/10.22033/ESGF/CMIP6.5271)

Canturk U and Kulaç Ş 2021 The effects of climate change scenarios on Tilia ssp. in Turkey *Environ. Monit. Assess.* **193** 1–15

Christian J I, Basara J B, Hunt E D, Otkin J A, Furtado J C, Mishra V, Xiao X and Randall R M 2021 Global distribution, trends, and drivers of flash drought occurrence *Nat. Commun.* **12** 6330

Consortium, E. C. E 2019a EC-Earth-Consortium EC-Earth3-Veg model output prepared for CMIP6 ScenarioMIP ssp245 *Earth System Grid Federation* (https://doi.org/10.22033/ESGF/CMIP6.4882)

Consortium, E. C. E 2019b EC-Earth-Consortium EC-Earth3-Veg model output prepared for CMIP6 ScenarioMIP ssp585 *Earth System Grid Federation* (https://doi.org/10.22033/ESGF/CMIP6.4914)

Consortium, E. C. E 2019c EC-Earth-Consortium EC-Earth3 model output prepared for CMIP6 ScenarioMIP ssp245 *Earth System Grid Federation* (https://doi.org/10.22033/ESGF/CMIP6.4880)

Consortium, E. C. E 2019d EC-Earth-Consortium EC-Earth3 model output prepared for CMIP6 ScenarioMIP ssp585 *Earth System Grid Federation* (https://doi.org/10.22033/ESGF/CMIP6.4912)

Cook B I, Mankin J S, Marvel K, Williams A P, Smerdon J E and Anchukaitis K J 2020 Twenty-first century drought projections in the CMIP6 forcing scenarios *Earth's Future* **8** e2019EF001461

Cook B I, Smerdon J E, Seager R and Coats S 2014 Global warming and 21st century drying *Clim. Dyn.* **43** 2607–27

Dai A, Zhao T and Chen J 2018 Climate change and drought: a precipitation and evaporation perspective *Current Climate Change Reports* **4** 301–12

Dix M *et al* 2019a CSIRO-ARCCSS ACCESS-CM2 model output prepared for CMIP6 ScenarioMIP ssp245 *Earth System Grid Federation* (https://doi.org/10.22033/ESGF/CMIP6.4321)

Dix M *et al* 2019b CSIRO-ARCCSS ACCESS-CM2 model output prepared for CMIP6 ScenarioMIP ssp585 *Earth System Grid Federation* (https://doi.org/10.22033/ESGF/CMIP6.4332)

Droogers P and Allen R G 2002 Estimating reference evapotranspiration under inaccurate data conditions *Irrigation and drainage systems* **16** 33–45

Feng S and Fu Q 2013 Expansion of global drylands under a warming climate *Atmos. Chem. Phys.* **13** 10081–94

Frierson D M W and Scheff J 2014 Scaling potential evapotranspiration with greenhouse warming *J. Clim.* **27** 1539–58

Funk C, Shukla S, Thiaw W M, Rowland J, Hoell A, Mcnally A, Husak G, Novella N, Budde M and Peters-Lidard C 2019 Recognizing the famine early warning systems network: over 30 years of drought early warning science advances and partnerships promoting global food security *Bull. Am. Meteorol. Soc.* **100** 1011–27

Green J K, Seneviratne S I, Berg A M, Findell K L, Hagemann S, Lawrence D M and Gentine P 2019 Large influence of soil moisture on long-term terrestrial carbon uptake *Nature* **565** 476–9

Guttman N B 1999 Accepting the standardized precipitation index: a calculation algorithm 1 *JAWRA Journal of the American Water Resources Association* **35** 311–22

Hance T, van Baaren J, Vernon P and Boivin G 2007 Impact of extreme temperatures on parasitoids in a climate change perspective *Annu. Rev. Entomol.* **52** 107–26

Hargreaves G H 1994 Defining and using reference evapotranspiration *Journal of Irrigation and Drainage Engineering* **120** 1132–9

Hayes M, Svoboda M, Wall N and Widhalm M 2011 The Lincoln declaration on drought indices: universal meteorological drought index recommended *Bull. Am. Meteorol. Soc.* **92** 485–8

Hui-Mean F, Yusop Z and Yusof F 2018 Drought analysis and water resource availability using standardised precipitation evapotranspiration index *Atmos. Res.* **201** 102–15

IPCC 2013 A Climate change 2013: the physical science basis *Contribution of working group I to the fifth assessment report of the intergovernmental panel on climate change* 1535

Jeong S-J, Schimel D, Frankenberg C, Drewry D T, Fisher J B, Verma M, Berry J A, Lee J-E and Joiner J 2017 Application of satellite solar-induced chlorophyll fluorescence to understanding large-scale variations in vegetation phenology and function over northern high latitude forests *Remote Sens. Environ.* **190** 178–87

Jiao W, Wang L, Smith W K, Chang Q, Wang H and D'odorico P 2021 Observed increasing water constraint on vegetation growth over the last three decades *Nat. Commun.* **12** 1–9

John J G *et al* 2018a NOAA-GFDL GFDL-ESM4 model output prepared for CMIP6 ScenarioMIP ssp245 *Earth System Grid Federation* (https://doi.org/10.22033/ESGF/CMIP6.8686)

John J G *et al* 2018b NOAA-GFDL GFDL-ESM4 model output prepared for CMIP6 ScenarioMIP ssp585 *Earth System Grid Federation* (https://doi.org/10.22033/ESGF/CMIP6.8706)

Li X, Li Y, Chen A, Gao M, Slette I J and Piao S 2019 The impact of the 2009/2010 drought on vegetation growth and terrestrial carbon balance in Southwest China *Agric. For. Meteorol.* **269** 239–48

Liu S C, Fu C, Shiu C J, Chen J P and Wu F 2009 Temperature dependence of global precipitation extremes *Geophys. Res. Lett.* **36**

Liu X, Li C, Zhao T and Han L 2020 Future changes of global potential evapotranspiration simulated from CMIP5 to CMIP6 models *Atmospheric and Oceanic Science Letters* **13** 568–75

Lloyd-Hughes B 2012 A spatio-temporal structure-based approach to drought characterisation *Int. J. Climatol.* **32** 406–18
Mckee T B, Doesken N J and Kleist J 1993 The relationship of drought frequency and duration to time scales *Proceedings of the 8th Conference on Applied Climatology* **17** 179–84
Mcvicar T R, Roderick M L, Donohue R J, LI L T, Thomas G V N, Thomas A, Grieser J, Jhajharia D, Himri Y and Mahowald N M 2012 Global review and synthesis of trends in observed terrestrial near-surface wind speeds: Implications for evaporation *J. Hydrol.* **416** 182–205
Van der Molen M K, Dolman A J, Ciais P, Eglin T, Gobron N, Law B E, Meir P, Peters W, Phillips O L and Reichstein M 2011 Drought and ecosystem carbon cycling *Agric. For. Meteorol.* **151** 765–73
O'neill B C, Tebaldi C, van Vuuren D P, Eyring V, Friedlingstein P, Hurtt G, Knutti R, Kriegler E, Lamarque J-F and Lowe J 2016 The scenario model intercomparison project (ScenarioMIP) for CMIP6 *Geoscientific Model Development* **9** 3461–82
Park S, Im J, Jang E and Rhee J 2016 Drought assessment and monitoring through blending of multi-sensor indices using machine learning approaches for different climate regions *Agricultural and Forest Meteorology* **216** 157–69
Pieper P, Düsterhus A and Baehr J 2020 A universal Standardized Precipitation Index candidate distribution function for observations and simulations *Hydrol. Earth Syst. Sci.* **24** 4541–65
Schupfner M *et al* 2019a DKRZ MPI-ESM1.2-HR model output prepared for CMIP6 ScenarioMIP ssp245 *Earth System Grid Federation* (https://doi.org/10.22033/ESGF/CMIP6.4398)
Schupfner M *et al* 2019b DKRZ MPI-ESM1.2-HR model output prepared for CMIP6 ScenarioMIP ssp585 *Earth System Grid Federation* (https://doi.org/10.22033/ESGF/CMIP6.4403)
Sherwood S and Fu Q 2014 A drier future? *Science* **343** 737–9
Shiogama H, Abe M and Tatebe H 2019a MIROC MIROC6 model output prepared for CMIP6 ScenarioMIP ssp245 *Earth System Grid Federation* (https://doi.org/10.22033/ESGF/CMIP6.5746)
Shiogama H, Abe M and Tatebe H 2019b MIROC MIROC6 model output prepared for CMIP6 ScenarioMIP ssp585 *Earth System Grid Federation* (https://doi.org/10.22033/ESGF/CMIP6.5771)
Song L, Li Y, Ren Y, Wu X, Guo B, Tang X, Shi W, Ma M, Han X and Zhao L 2019 Divergent vegetation responses to extreme spring and summer droughts in Southwestern China *Agric. For. Meteorol.* **279** 107703
Streel D E *et al* 2022 Regional climate moderately influences species-mixing effect on tree growth-climate relationships and drought resistance for beech and pine across Europe *Forest Ecology and Management* **520** 120317
Sun S, Chen H, Wang G, Li J, Mu M, Yan G, Xu B, Huang J, Wang J and Zhang F 2016 Shift in potential evapotranspiration and its implications for dryness/wetness over Southwest China *Journal of Geophysical Research: Atmospheres* **121** 9342–55
Swart N C *et al* 2019a CCCma CanESM5 model output prepared for CMIP6 ScenarioMIP ssp245 *Earth System Grid Federation* (https://doi.org/10.22033/ESGF/CMIP6.3685)
Swart N C *et al* 2019b CCCma CanESM5 model output prepared for CMIP6 ScenarioMIP ssp585 *Earth System Grid Federation* (https://doi.org/10.22033/ESGF/CMIP6.3696)
Thornthwaite C W 1948 An approach toward a rational classification of climate *Geographical review* **38** 55–94
Trenberth K E, Dai A, van der Schrier G, Jones P D, Barichivich J, Briffa K R and Sheffield J 2014 Global warming and changes in drought *Nat. Clim. Change* **4** 17–22
Ukkola A M, De Kauwe M, Roderick M, Abramowitz G and Pitman A 2020 Robust future changes in meteorological drought in cmip6 projections despite uncertainty in precipitation *Geophys. Res. Lett.* **47** (11) e2020GL087820
Vicente-Serrano S M, BEGUERÍA S and LóPEZ-Moreno J I 2010 A multiscalar drought index sensitive to global warming: the standardized precipitation evapotranspiration index *J. Clim.* **23** 1696–718
Vicente-Serrano S M, Van der Schrier G, BEGUERÍA S, Azorin-Molina C and Lopez-Moreno J-I 2015 Contribution of precipitation and reference evapotranspiration to drought indices under different climates *J. Hydrol.* **526** 42–54
Volodin E *et al* 2019a INM INM-CM4-8 model output prepared for CMIP6 ScenarioMIP ssp245 *Earth System Grid Federation* (https://doi.org/10.22033/ESGF/CMIP6.12327)
Volodin E *et al* 2019b INM INM-CM4-8 model output prepared for CMIP6 ScenarioMIP ssp585 *Earth System Grid Federation* (https://doi.org/10.22033/ESGF/CMIP6.12337)
Volodin E *et al* 2019c INM INM-CM5-0 model output prepared for CMIP6 ScenarioMIP ssp245 *Earth System Grid Federation* (https://doi.org/10.22033/ESGF/CMIP6.12328)
Volodin E *et al* 2019d INM INM-CM5-0 model output prepared for CMIP6 ScenarioMIP ssp585 *Earth System Grid Federation* (https://doi.org/10.22033/ESGF/CMIP6.12338)
Wang M, Ding Z, Wu C, Song L, Ma M, Yu P, Lu B and Tang X 2021 Divergent responses of ecosystem water-use efficiency to extreme seasonal droughts in Southwest China *Sci. Total Environ.* **760** 143427
Wang R, Li L, Chen L, Ning L, Yuan L and Lü G 2022 Respective contributions of precipitation and potential evapotranspiration to long-term changes in global drought duration and intensity *Int. J. Climatol.*
Wang Y, Xu Y, Lei C, Li G, Han L, Song S, Yang L and Deng X 2016 Spatio-temporal characteristics of precipitation and dryness/wetness in yangtze river delta, eastern China, during 1960–2012 *Atmos. Res.* **172** 196–205
Wieners K-H *et al* 2019a MPI-M MPI-ESM1.2-LR model output prepared for CMIP6 ScenarioMIP ssp245 *Earth System Grid Federation* (https://doi.org/10.22033/ESGF/CMIP6.6693)
Wieners K-H *et al* 2019b MPI-M MPI-ESM1.2-LR model output prepared for CMIP6 ScenarioMIP ssp585 *Earth System Grid Federation* (https://doi.org/10.22033/ESGF/CMIP6.6705)
Wu G, Chen J, Shi X, Kim J S, Xia J and Zhang L 2022 Impacts of global climate warming on meteorological and hydrological droughts and their propagations *Earth's Future* **10** e2021EF002542
Wu J and Chen X 2019 Spatiotemporal trends of dryness/wetness duration and severity: The respective contribution of precipitation and temperature *Atmos. Res.* **216** 176–85
Xin X, Wu T, Shi X, Zhang F, Li J, Chu M, Liu Q, Yan J, Ma Q and Wei M 2019a BCC BCC-CSM2MR model output prepared for CMIP6 ScenarioMIP ssp245 *Earth System Grid Federation* (https://doi.org/10.22033/ESGF/CMIP6.3030)
Xin X, Wu T, Shi X, Zhang F, Li J, Chu M, Liu Q, Yan J, Ma Q and Wei M 2019b BCC BCC-CSM2MR model output prepared for CMIP6 ScenarioMIP ssp585 *Earth System Grid Federation* (https://doi.org/10.22033/ESGF/CMIP6.3050)
Xin X, Wu T, Zhang J, Yao J and Fang Y 2020 Comparison of CMIP6 and CMIP5 simulations of precipitation in China and the East Asian summer monsoon *Int. J. Climatol.* **40** 6423–40
Xu K, Yang D, Yang H, Li Z, Qin Y and Shen Y J J O H 2015 Spatio-temporal variation of drought in China during 1961–2012: a climatic perspective *J. Hydrol.* **526** 253–64
Xu L, Chen N, Yang C, Zhang C, Yu H J A and Meteorology F 2021a A parametric multivariate drought index for drought monitoring and assessment under climate change *Agricultural and Forest Meteorology* **310** 108657

Xu Y, Zhang X, Hao Z, Hao F and Li C 2021b Projections of future meteorological droughts in China under CMIP6 from a three-dimensional perspective *Agric. Water Manage.* **252** 106849

Yang Y, Chen R, Yin G, Wang C, Liu G, Verger A, Descals A, Filella I and Penuelas J 2022 Divergent performances of vegetation indices in extracting photosynthetic phenology for northern deciduous broadleaf forests *IEEE Geosci. Remote Sens. Lett.* **19** 1–5

Yu Y 2019a CAS FGOALS-f3-L model output prepared for CMIP6 ScenarioMIP ssp245 *Earth System Grid Federation* (https://doi.org/10.22033/ESGF/CMIP6.3468)

Yu Y 2019b CAS FGOALS-f3-L model output prepared for CMIP6 ScenarioMIP ssp585 *Earth System Grid Federation* (https://doi.org/10.22033/ESGF/CMIP6.3502)

Yukimoto S *et al* 2019a MRI MRI-ESM2.0 model output prepared for CMIP6 ScenarioMIP ssp245 *Earth System Grid Federation* (https://doi.org/10.22033/ESGF/CMIP6.6910)

Yukimoto S *et al* 2019b MRI MRI-ESM2.0 model output prepared for CMIP6 ScenarioMIP ssp585 *Earth System Grid Federation* (https://doi.org/10.22033/ESGF/CMIP6.6929)

Zelinka M D, Myers T A, Mccoy D T, Po-Chedley S, Caldwell P M, Ceppi P, Klein S A and Taylor K E 2020 Causes of higher climate sensitivity in CMIP6 models *Geophysical Research Letters* **47** e2019GL085782

Zeng P, Sun F, Liu Y and Che Y 2020 Future river basin health assessment through reliability-resilience-vulnerability: Thresholds of multiple dryness conditions *Sci. Total Environ.* **741** 140395

Zeng Z *et al* 2021 *Legacy effects of spring phenology on vegetation growth under preseason meteorological drought in the Northern Hemisphere* **310** 108630

Zhang J, Sun F, Lai W, Lim W H, Liu W, Wang T and Wang P 2019 Attributing changes in future extreme droughts based on PDSI in China *J. Hydrol.* **573** 607–15

Zhang Y, Commane R, Zhou S, Williams A P and Gentine P 2020 Light limitation regulates the response of autumn terrestrial carbon uptake to warming *Nat. Clim. Change* **10** 739–43

Zhao T and Dai A 2015 The magnitude and causes of global drought changes in the twenty-first century under a low–moderate emissions scenario *J. Clim.* **28** 4490–512

Zhao T and Dai A 2021 CMIP6 Model-projected Hydroclimatic and drought changes and their causes in the 21st century *J. Clim.* **35** 897–921

Ziehn T *et al* 2019a CSIRO ACCESS-ESM1.5 model output prepared for CMIP6 ScenarioMIP ssp245 *Earth System Grid Federation* (https://doi.org/10.22033/ESGF/CMIP6.4322)

Ziehn T *et al* 2019b CSIRO ACCESS-ESM1.5 model output prepared for CMIP6 ScenarioMIP ssp585 *Earth System Grid Federation* (https://doi.org/10.22033/ESGF/CMIP6.4333)